IEEE Photonics Journal
An IEEE Photonics Society Publication

Sensing Characterization of Helical Long Period Fiber Grating Fabricated by a Double-Side CO_2 Laser in Single-Mode Fiber

Volume 11, Number 3, June 2019

Yujian Li
Ping Lu
Chi Zhang
Wenjun Ni
Deming Liu
Jiangshan Zhang

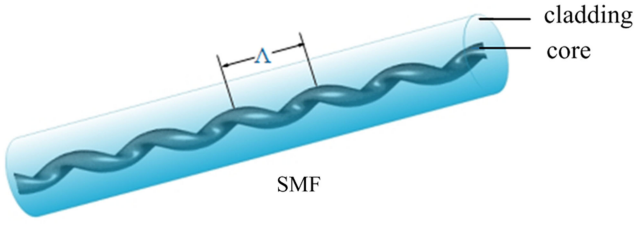

DOI: 10.1109/JPHOT.2019.2913700
1943-0655

Sensing Characterization of Helical Long Period Fiber Grating Fabricated by a Double-Side CO_2 Laser in Single-Mode Fiber

Yujian Li,[1] Ping Lu,[1] Chi Zhang,[1] Wenjun Ni,[1] Deming Liu,[1] and Jiangshan Zhang[2]

[1]School of Optical and Electronic Information, National Engineering Laboratory for Next Generation Internet Access System, Huazhong University of Science and Technology, Wuhan 430074, China
[2]Department of Electronics and Information Engineering, Huazhong University of Science and Technology, Wuhan 430074, China

DOI:10.1109/JPHOT.2019.2913700

Manuscript received January 31, 2019; revised March 28, 2019; accepted April 24, 2019. Date of publication April 29, 2019; date of current version May 14, 2019. This work was supported in part by the National Natural Science Foundation of China under Grant 61775070 and in part by the National Key R&D Program of China under Grant 2018YFF01011800. Corresponding author: P. Lu (e-mail: pluriver@mail.hust.edu.cn).

Abstract: A simple and efficient manufacture method of helical long period fiber grating (HLPFG) in a single-mode fiber (SMF) is designed and verified through experiment. Different from the previous fabricating methods, the SMF is heated by a double-side CO_2 laser beam after being twisted. There are multiple transmission depletions caused by model coupling which could be observed when the period length is 500 μm. The sensing characteristics of the HLPFG have been investigated. Experimental results demonstrate axial strain sensitivities of 3.3 and 6.4 pm/$\mu\varepsilon$ at the selected dips in the range of 0–450 $\mu\varepsilon$ or temperature sensitivities of 35.3 and 49.5 pm/°C at the selected dips in the range of 20–70 °C, respectively. Moreover, through theoretical analysis, it is found that the fabricated HLPFG can measure axial strain and temperature concurrently by monitoring the resonance wavelength shift. Therefore, the fabricated HLPFG has brilliant applications value in dual measurement.

Index Terms: Helical long period fiber grating, axial strain, temperature, simultaneous measurement.

1. Introduction

During the past several decades, optical fiber sensors (OFSs) have exhibited significant potential in environmental monitoring, resource exploration, and biomedical field owing to their superiority of long life, fast response, high accuracy, no electromagnetic induction, compact size over traditional sensors and resistance to chemical corrosion, etc. [1]. A variety of OFSs have been proposed and widely applied for different realms. Among these, the long period fiber grating (LPFG) has been extensively researched for its high sensitivity to external environment. Once the phase-matching condition is met, the LPFG has ability to couple fundamental core mode to the forward propagating cladding mode [1]. The idea that the LPFGs can be used as a sensor was first given by Vengsarkar *et al.* [2]. Then the LPFGs are under intensive investigation in sensing variation in the external

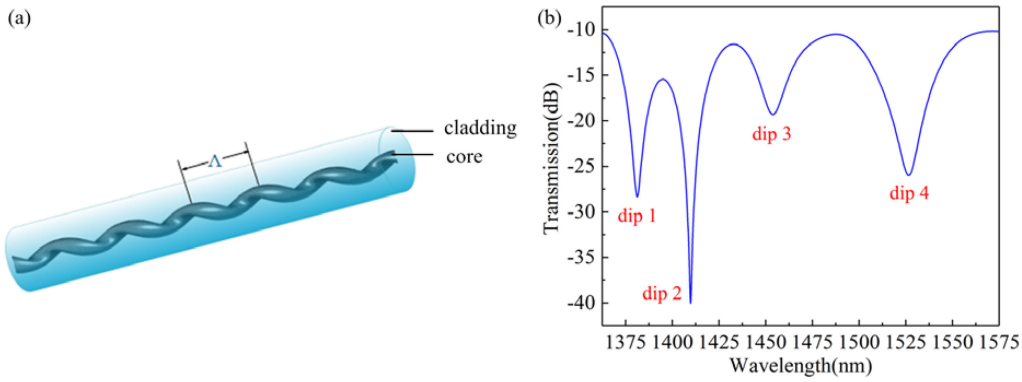

Fig. 1. (a) Sketches of the HLPFG. (b) The transmission spectrum of the fabricated HLPFG.

environment [3], [4]. For example, a LPFG inscribed in a photonic crystal fiber (PCF) was proposed and a strain sensitivity of -0.19 pm/$\mu\varepsilon$ and a temperature sensitivity of 10.9 pm/°C were obtained in Ref [5]. A strain sensitive LPFG sensor is discussed in Ref [6]. Sensitivity of this sensor is found to be 0.931 pm/$\mu\varepsilon$. A twist sensor based on corrugated LPFG was proposed by L. A. Wang, whose sensitivity is 36 pm/(rad/m) [7]. Jieliang Li *et al.* proposed a structure that a LPFG cascaded to an S structure, of which wavelength sensitivity is -52.57 nm/RIU in the scale of 1.33 to 1.37 [8]. Though the LPFGs have the capacity for sensing the external environment, the sensitivity of it is not very high.

To enhance the sensitivity of LPFGs, various improved structures including the phase shift LPFG (PS-LPFG) [9], cascaded LPFG [10], ultra-LPFG [11] and helical long period gratings (HLPFG) have been reported to date. The mechanical strength of the cascaded LPFG is very low, which is not conducive to practical applications. The ultra-LPFG and the PS-LPFG are difficult to fabricate. As shown in Fig. 1(a), where the HLPFGs different from conventional LPFGs is that the HLPFGs have a periodic helical refractive index modulation in the fiber core area. A HLPFG with a high sensitivity of 117.4 pm/(rad/m) in the twist range from 0 to 105 rad/m was fabricated by femtosecond laser in SMF [12]. A HLPFG with a strain sensitivity of 1.5 pm/$\mu\varepsilon$ in the scale of 0 to 1400 $\mu\varepsilon$ was proposed in [13]. The HLPFGs fabricated in [22] have sensitivity of -2321.67 nm/RIU when measuring the refractive index. It is obvious that the sensing performance of HLPFG is better than traditional LPFGs both in measurement range and sensitivity. The HLPFGs were first fabricated by Poole *et al.* in a two-mode fiber [14]. X. P. Wang *et al.* has presented a new system for HLPFG fabrication, in which a single-side CO_2 laser is used [16]. The quality of the HLPFG fabricated by this method is uneven because of the unilateral heating. Other people used a point-by-point etching method, which only allows a portion of the fiber to be heated and can only twist the fiber at a small angle, resulting in the grating etching depth is insufficient [15]. All the methods mentioned above were heating and twisting the fiber in the meantime, causing deform to the HLPFG structure and reducing the detection sensitivity of the HLPFG.

In this paper, a new, simple, highly controllable method of fabricating HLPFG have been proposed and demonstrated through experiments. In addition, the sensing properties of the fabricated HLPFG on temperature and axial strain are investigated through experiments. From the experimental data can be derived that the HLPFG has temperature wavelength sensitivity of 49.5 pm/°C and 35.5 pm/°C at different interference dips in the range from 20 to 70 °C. Moreover, the HLPFG realizes axial strain wavelength sensitivity of 6.4 pm/$\mu\varepsilon$ and 3.3 pm/$\mu\varepsilon$ in the scale of 0 to 450 $\mu\varepsilon$. Though the HLPFG exhibits high sensitivity, it is susceptible to temperature cross-sensitivity, which is analogous to LPFGs. The commonly used ways to solve this problem are using temperature compensation system and dual-parameter measurement. In this work, the experimental findings have indicated the fabricated HLPFG can simultaneously measure temperature and strain by using the coefficient matrix. Therefore, the proposed HLPFGs have the superiority of inexpensive,

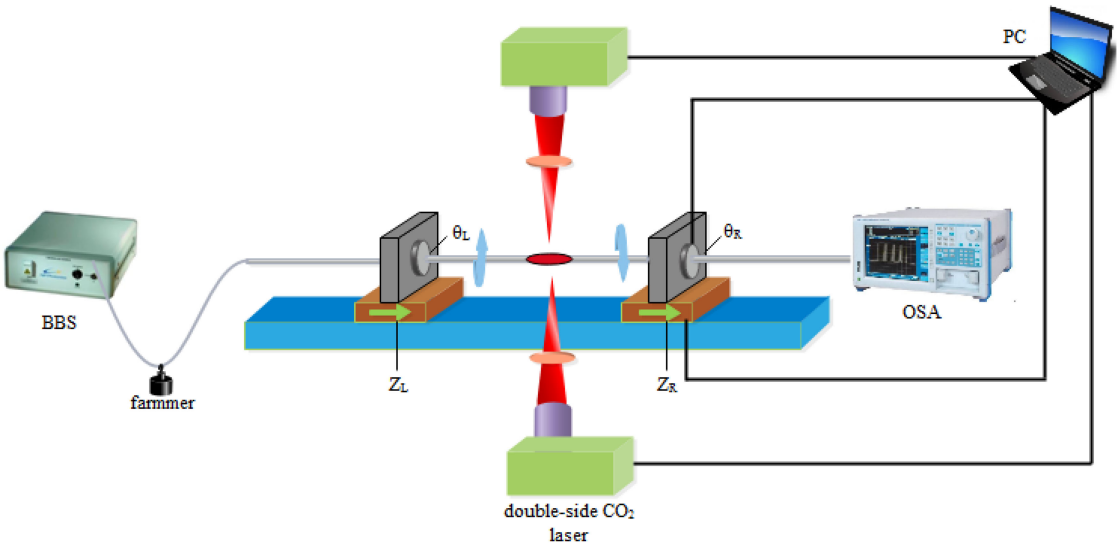

Fig. 2. The experimental device for fabrication of the HLPFG.

simple preparation process and good structure stability, and its application prospect in many fields is tantalizing.

2. Fabrication

There always exists a small amount of random core-cladding eccentricity between the SMF core and cladding because of fabrication imperfection [21]. Therefore, the heating twist process will make the core into a helical structure and then spirally modulate the index of fiber core. Fig. 2 shows the sample schematic diagram of the experimental device for fabricating the HLPFGs. Two ends of SMF are fixed on the displacement platform with two rotation motors by the fiber holders. The velocity of two translation stages and the two rotation motors and the direction of the two rotation motors could be set by computer software. It is well to be reminded that a small weight of $\sim$5 g is used to provide a small axial tension to make sure the SMF is stretched horizontally during the grating fabrication. In traditional processing methods, the SMFs were usually irradiated by the CO_2 laser on one side. As is well known, the light power on the laser incident side is bigger than that on the laser escape side [26], which can easily produce uneven heating of the optical fiber and thus cause the fiber to bend slightly. To avoid this problem, the double-side CO_2 laser irradiation is used in this system, ensuring the accuracy and consistency of grating writing. To make sure the fabrication of the HLPFG is successful, an optical broadband source (BBS) and an optical spectrum analyzer (OSA) were utilized to monitor the changes of transmission spectrum during the fabrication process.

HLPFGs were fabricated by method of twisting SMFs while heating, exposing to CO_2 laser in Ref. [16], which is easily to deform the optical fiber and a stepped structure is formed to increase the loss. To solve this problem, a new fabrication method is designed that the heating process is after the twisting process when etching one period of the grating. As is shown in Table 1, in the 0 to 3 seconds of the fabrication, the left-hand rotary motor θ_L and the right-hand rotary motor θ_R are each rotated by 180° in the opposite direction individually, which corresponds to the introduction of 360° twists in the entire optical fiber. The speed of the rotation motor is 0.060°/ms. After three seconds, the double-side CO_2 laser begins to irradiate the SMF to write the Pre-twist into the optical fiber. While the SMF is heated, the actuator translates the fiber by the length of one grating period along its axis. So far, a period of the grating is etched on the fiber. After repeating the above process N times, the length of the fabricated HLPFG is $L = N\Lambda$, the Λ is the pitch of HLPFG. The grating pitch can be calculated according to the formula: $\Lambda = \upsilon t$; υ is the speed of translation stage; t is the time

TABLE 1
State of the Motor and the Laser at Different Times During the Fabrication Process

Time		0~3s	3s later
Light conditions		No light	Light get through (standard power)
Motor direction	θ_L	Turning in the opposite directions	Keeping still
	θ_R		
	ZL	Keeping still	Moving in the same direction
	ZR		

of CO_2 laser irradiation. Thus, Λ can be precisely adjusted by changing the υ and t. Based on the experimental results, the parameters that can affect the quality of the grating has been optimized through a series of experiments. The length between the two fiber fixtures is 50 mm, the output power of the CO_2 laser is about 580 bit (16.2W) and spot beam radius is 2 mm.

Experiments show that this writing method is feasible, simple, efficient and highly controllable. By using the proposed method, HLPFGs of arbitrary periods and length for specific application scenarios can be easily obtained.

It is well known that the period of the HLPFG affects resonance wavelength [17]. The number of the period has great effect on the coupling efficiency of the HLPFG. On the one hand, only very few cladding modes can couple with the core mode if the N is too small. On the other hand, an ultra-long grating length will lead to large insertion and difficulty on fabricating. Therefore, the period of the HLPFG Λ and the number of period L should be carefully considered before fabricating. After several trails, the Λ and the N are selected to be 500 μm and 50, respectively. Fig. 1(b) shows the transmission spectrum through the fabricated HLPFG, in which several attenuation dips can be observed. For the convenience of description, these dips are named dip 1, dip 2, dip 3 and dip 4. Compared to prior LPFGs, the fabricated HLPFG show a relatively high insert loss of $\sim$11 dB. One possible reason is that the micro-bending effects are imbedded in HLPFG due to the axial tension produced in twisting process [25].

3. Principles

Similar to conventional LPFGs [12], [13], the HLPFGs is capable of coupling the fundamental core mode to the forward propagating cladding modes when the phase-matching condition is met. The resonant wavelengths can be expressed as [16]:

$$\lambda_B = (n_{eff}^{co} - n_{eff}^{cl})\Lambda \tag{1}$$

Where λ_B is the resonant wavelength, n_{eff}^{co} is the effective refractive index of fundamental mode, n_{eff}^{cl} is the effective refractive index of cladding mode and Λ is the period of grating. Beyond that, mode coupling occurs not only between the fundamental core mode LP_{01} and cladding mode LP_{0m}, but also between LP_{lm}, where $l > 1$ and $m > 1$ [19]. Therefore, multiple resonant wavelengths would be recognized in the transmission spectrum. In particular, n_{eff}^{co}, n_{eff}^{cl} and Λ are susceptible to the temperature or axial strain change, leading to the resonant wavelength shift [17].

When the HLPFG is applied axial strains, the material refractive index will change duo to elasto-optical effect, which could be calculated by [23]:

$$n_i^{\varepsilon} = n_i - \frac{1}{2} n_i^3 [p_{12} - \mu(p_{11} + p_{12})](\varepsilon - \varepsilon_0)\beta \quad (i = 1, 2) \tag{2}$$

Where n_1 represents the effective refractive index of core and n_2 represents the effective refractive index of cladding. p_{11} and p_{12} are the Pockel coefficients of fiber and μ is Poisson ratio. Considering

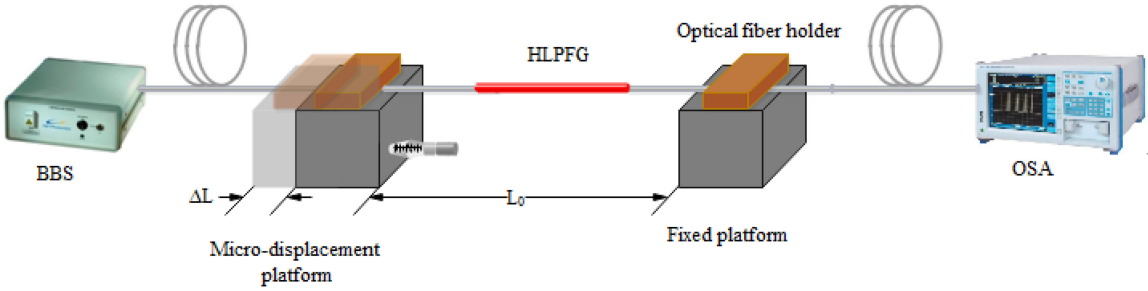

Fig. 3. Diagram of the strain experimental set up.

the unevenness and discontinuity of fiber materials, the distribution of axial strain on the cross section of the fiber is not uniform. β is strain distribution coefficient. Its value is related to the distance from the axial and the type of material [18]. $\beta = 1$ when calculating the cladding refractive index change while $\beta < 1$ when calculating the core refractive index change. Theoretically, the Λ will vary under the action of axial strain. For clarity, the Eqs.(1) can be converted into functions of axial strains as Eqs.(3a) and (3c):

$$\Delta n_\varepsilon = n_1^\varepsilon - n_2^\varepsilon \tag{3a}$$

$$\Lambda_\varepsilon = \Lambda[1 + \eta(\varepsilon - \varepsilon_0)] \tag{3b}$$

$$\lambda_B^\varepsilon = \Delta n_\varepsilon \Lambda_\varepsilon \tag{3c}$$

Where η is the strain extend coefficient of the fiber. The η and β should be tested by experiment. Thus, the theoretical axial strain sensitivity can be calculated by using the above formula.

As the temperature changes, the transmission spectrum shift is mainly affected by the thermal-expansion effect and the thermo-optical effect. The above formula can be expressed as follows:

$$\Delta n_T = (n_{eff}^{co} - n_{eff}^{cl})[1 + \xi(T - T_0)] \tag{4a}$$

$$\Lambda_T = \Lambda[1 + \alpha(T - T_0)] \tag{4b}$$

$$\lambda_B^T = \Delta n_T \Lambda_T \tag{4c}$$

For ordinary single mode fiber, the thermal-expansion coefficient is $\alpha = 5.5 \times 10^{-7}\,^\circ C$ and the thermo-optical coefficient is $\zeta = 7.5 \times 10^{-6}\,^\circ C$. Take dip 4 as an example, the resonant wavelength of dip 4 is 1525 nm, the Λ is 500 μm, so $\Delta n = n_{eff}^{co} - n_{eff}^{cl} = 3.05 \times 10^{-3}$. The theoretical temperature sensitivity is 12.3 pm/°C. That is, the transmission spectrum will be red-shift when the temperature rises.

In the approximate model, many factors that affect the sensitivity are not being considered, such as the accurate refractive index distribution of the helical structure, uniformity of the grating structure [23]. Beyond that, α, ζ and η might change during the high-temperature process [23]. Thus, there may be slight deviation between the theoretical sensitivity and the sensitivity obtained by experiment.

4. Experimental Results and Discuss

4.1 Strain Experiment

The axial strain measurement device is shown in Fig. 3. An optical BBS with wavelength range from 600 nm to1700 nm is used as the light source and a high resolution OSA is utilized to trace the transmitted spectrum. It's also worth mentioning that the room temperature of 25 °C was maintained during the whole process of strain measurement. Two ends of the HLPFG are mounted on a high precision displacement platform with 10 μm resolution. During the course of the experiment, axial strain would be applied on the HLPFG by moving the micro-displacement platform. The axial strain

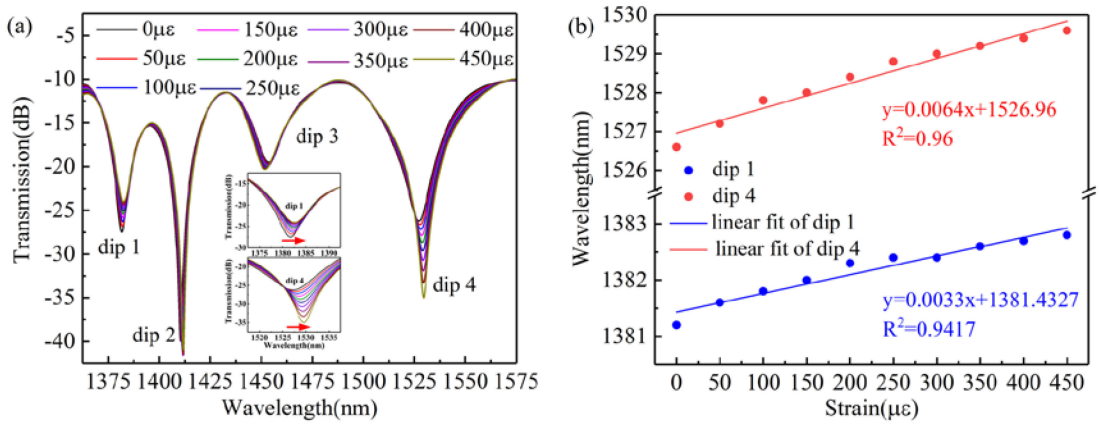

Fig. 4. (a) The HLPFG's transmitted spectrum at different axial strain conditions. (b) The fitting curve about the resonant wavelength under different axial strain at dip 1 and dip 4.

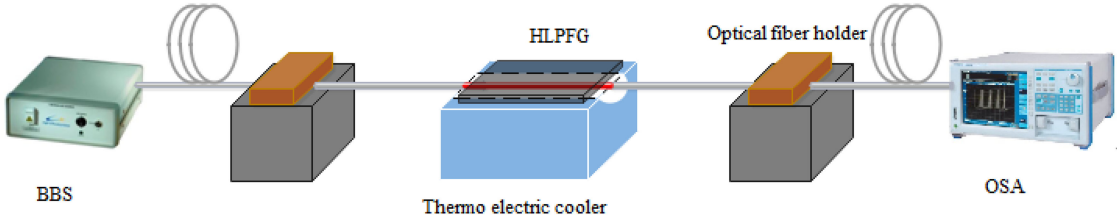

Fig. 5. Diagram of the temperature experimental apparatus.

exerted on the HLPFG can be expressed as $\varepsilon_0 = \Delta L / L_0$. Where L_0 is the initial distance between the two platforms and $L_0 = 20$ mm, ΔL is the axial displacement of moveable platform. Therefore, there will be 50 $\mu\varepsilon$ axial strain exerted on the HLPFG when the micro-displacement platform moving 10 μm. The transmission spectrum of the HLPFG under different axial strains in the range from 0 to 450 $\mu\varepsilon$ is shown in Fig. 4(a). The transmission spectrum shifts to long wavelength with the increase of the axial strains. Dip 1 and dip 4 are being chosen as the observation point because they have high sensitivities to axial strains change. The corresponding fitting curve about the resonant wavelength and the axial strain at dip 1 and dip 4 are shown in Fig. 4(b). Experimental results achieve strain sensitivities of 3.3 pm/$\mu\varepsilon$ at dip 1 and 6.4 pm/$\mu\varepsilon$ at dip 4 respectively, which is higher than the conventional LPFGs. The strain sensitivity of the HLPFG fabricated by the proposed method is three times that of the grating prepared by other methods in Ref. [27].

4.2 Temperature Experiment

Fig. 5. shows the diagram of experimental equipment for temperature measurement. The temperature change is carried out by employing a Thermoelectric Cooler (TEC), where the temperature is well controlled ranging from 20 °C to 70 °C at 0.1 °C per step. Fig. 6(a) shows the transmission spectrum of the HLPFG at different temperature. To ensure the accuracy of the measurement, each transmission spectrum is recorded after the TEC has stabilized for 15 minutes. The transmission spectrum shows a red shift when temperature going up. Dip 1 and dip 4 are also being chosen as the observation point. The corresponding fitting curve about the resonant wavelength of dip 1 and dip 4 with the increase of the temperature is shown in Fig. 6(b), which indicates that the resonance wavelength of HLPFG varies with temperature monotonically and linearly. The temperature sensitivities of 35.3 pm/ °C at dip 1 and 49.5 pm/ °C at dip 4 are achieved. Clearly, compared with ordinary LPFG, the fabricated HLPFGs have higher temperature sensitivity.

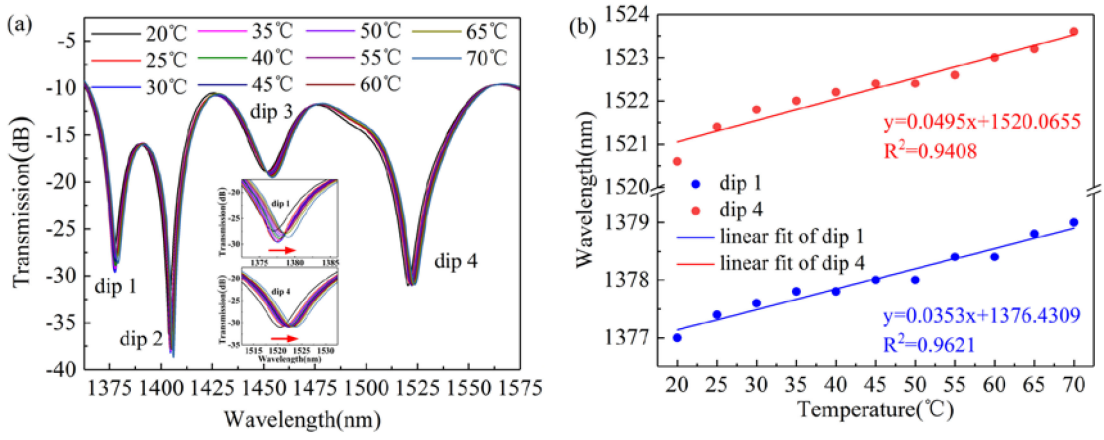

Fig. 6. (a) The HLPFG's transmitted spectrum at different temperature conditions. (b) The fitting curve about the resonant wavelength under different temperature at dip 1 and dip 4.

4.3 Simultaneous Strain and Temperature Measurement

From the Figs. 4 and 6, the resonant wavelength of dip 1 and dip 4 shift as a linear function of axial strain and temperature. And there exist sensitivity difference between the dip 1 and dip 4 when the axial strain or temperature changes. Hence, dip 1 and dip 4 can be used to simultaneously measure temperature and strain. The resonant wavelength sensitivities of axial strain at dip 1 and dip 4 are set to $K\varepsilon\ 1$ and $K\varepsilon\ 4$. The resonant wavelength of temperature at dip 1 and dip 4 are set to $KT\ 1$ and $KT\ 4$. When the axial strain applied to the HLPFG changes simultaneously with the external temperature, the cross-sensitivity of the resonant wavelength can be given in a matrix form as

$$\begin{pmatrix} \Delta\lambda_1 \\ \Delta\lambda_4 \end{pmatrix} = \begin{pmatrix} K_1^{\varepsilon} & K_1^{T} \\ K_4^{\varepsilon} & K_4^{T} \end{pmatrix} \begin{pmatrix} \Delta\varepsilon \\ \Delta T \end{pmatrix} \tag{5}$$

Where $\Delta\lambda_1$ is the wavelength shift of dip 1 and $\Delta\lambda_4$ is the wavelength shift of dip 4. The volume changes of strain and temperature change are $\Delta\varepsilon$ and ΔT, respectively. According to the previous experimental results, $K\varepsilon\ 1 = 3.3$ pm/$\mu\varepsilon$, $K\varepsilon\ 4 = 6.4$ pm/$\mu\varepsilon$, KT 1 = 35.3 pm/ °C, KT 4 = 49.5 pm/ °C.

$$\begin{pmatrix} \Delta\varepsilon \\ \Delta T \end{pmatrix} = \frac{1}{-62.6} \begin{pmatrix} 49.5 & -35.3 \\ -6.4 & 3.3 \end{pmatrix} \begin{pmatrix} \Delta\lambda_1 \\ \Delta\lambda_4 \end{pmatrix} \tag{6}$$

In the above measurement matrix, the unit of the wavelength, strain and temperature are nanometer, micro strain and degree centigrade, respectively. As can be seen, when temperature and axial strains are simultaneously applied on the HLPFGs, the changes of the measured parameters can be easily calculated according to the transmission spectrum changes and the sensitivity matrix. During the measurement process, the OSA's resolution is set to be 0.02 nm. According to Eqs. (6), the theoretical resolution of temperature within range of 20 to 70 °C and axial strain within range of 0 to 450 $\mu\varepsilon$ is 0.99 °C and 4.53 $\mu\varepsilon$, respectively.

In view of the above results, it can be concluded that the fabricated HLPFG can not only response to external environmental axial strain and temperature changes but also cut the error arising from the temperature cross-sensitivity in strain.

5. Conclusion

In summary, a new approach to fabricating the HLPFG in conventional SMF was proposed and experimentally demonstrated. Different from the previous method, the new fabricating method gives priority to twisting the single mode fiber to heating it. By using this method, high quality HLPFGs as

a strain sensor with sensitivities of 3.3 pm/$\mu\varepsilon$ and 6.4 pm/$\mu\varepsilon$ at the selected dips in the range of 0 to 450 $\mu\varepsilon$ or a temperature sensor with sensitivities of 35.3 pm/ °C and 49.4 pm/ °C at the selected dips in the range of 20 to 70 °C can be obtained. Beyond that, the possibility of measurement of using the fabricated HLPFG to measure strain and temperature in the meantime has been verified through theoretical analysis. By monitoring the resonance wavelength shift and calculating through the cross-matrix, the fabricated HLPFG can be used for dual-parameter measurement. Theoretical resolutions of dual-parameter measurement are $\pm$4.53 $\mu\varepsilon$ and $\pm$0.99 °C. Overall, the proposed method to fabricate HLPFG is easy to implement and low cost. The fabricated HLPFG has brilliant applications value in various fields, such as auto industry, border security and parts manufacturing.

References

[1] B. Lee, "Review of the present status of optical fiber sensors," *Opt. Fiber Technol.*, vol. 9, no. 2, pp. 57–79, Apr. 2003.
[2] A. M. Vengsarkar, P. J. Lemaire, J. B. Judkins, V. Bhatia, T. Erdogan, and J. E. Sipe, "Hybrid fibre Bragg grating/LPG for strain/temperature measurement," *J. Lightw. Technol.*, vol. 14, no. 58, pp. 58–64, Jan. 1996.
[3] V. Bhatia and A. M. Vengsarkar, "Optical fiber long-period grating sensors," *Opt. Lett.*, vol. 21, pp. 692–694, 1996.
[4] H. J. Patrick, C. C. Chang, and S. T. Vohra, "Long period fiber gratings for structural bend sensing," *Electron. Lett.*, vol. 34, pp. 1773–1775, Sep. 1998.
[5] Y. Zhu, P. Shum, H. W. Bay, M. Yan, X. Yu, and J. Hu, "Strain-insensitive and high-temperature long-period gratings inscribed in photonic crystal fiber," *Opt. Lett.*, vol. 30, no. 4, pp. 367–369, 2005.
[6] B. A. Tahir *et al.*, "Long-period grating as strain sensor," *J. Ovonic Res.*, vol. 8, no. 5, pp. 113–120, Oct. 2012.
[7] L. A. Wang, C. Y. Lin, and G. W. Chern, "A torsion sensor made of a corrugated long period fibre grating," *Meas. Sci. Technol.*, vol. 12, pp. 793–799, 2001.
[8] J. Li, W. Zhang, and S. Gao, "Long-period fiber grating cascaded to an S fiber taper for simultaneous measurement of temperature and refractive index," *IEEE Photon. Technol. Lett.*, vol. 25, no. 9, pp. 888–891, May 2013.
[9] W. Yang, T. Geng, and J. Yang, "A phase-shifted long period fiber grating based on filament heating method for simultaneous measurement of strain and temperature," *J. Opt.*, vol. 17 no. 7, pp. 075801–075807, 2015.
[10] L. Wang *et al.*, "Torsion sensor based on two cascaded long period fiber gratings fabricated by CO_2 laser pulse irradiation and HF etching technique respectively," *J. Mod. Opt.*, vol. 64, pp. 1–5, 2016.
[11] Y. J. Rao, T. Zhu, and Q. J. Mo, "Highly sensitive fiber-optic torsion sensor based on an ultra-long-period fiber grating," *Opt. Commun.*, vol. 266, no. 1, pp. 187–190, 2006.
[12] G. Shvets, S. Trendafilov, V. I. Kopp, D. Neugroschl, and A. Z. Genack, "Polarization properties of chiral fiber gratings," *J. Opt. A, Pure Appl.*, vol. 11, no. 7, Oct. 2009, Art. no. 074007.
[13] J. R. Qian, J. Su, L. L. Xue, and L. Yang, "Coupled-mode analysis for chiral fiber long-period gratings using local mode approach," *IEEE J. Quantum Electron.*, vol. 48, no. 1, pp. 49–55, Jan. 2012.
[14] C. D. Poole, C. D. Townsend, and K. T. Nelson, "Helical-grating two-mode fiber spatial-mode coupler," *J. Lightw. Technol.*, vol. 9, no. 5, pp. 598–604, May 1991.
[15] S. Oh, K. R. Lee, U. C. Peak, and Y. Chung, "Fabrication of helical long-period fiber gratings by use of a CO_2 laser," *Opt. Lett.*, vol. 29, no. 13, pp. 1464–1466, Jan. 2004.
[16] X. P. Wang, D. D. Wang, and Q. Wang, "Fabrication and characterization of helical long-period fiber gratings in single-mode fibers," *Optik*, vol. 158, pp. 28–32, 2018.
[17] R. Gao, Y. Jiang, and L. Jiang, "Multi-phase-shifted helical long period fiber grating based temperature-insensitive optical twist sensor," *Opt. Exp.*, vol. 22, no. 13, pp. 15697–15709, Jun. 2014.
[18] K. Ren *et al.*, "Online fabrication scheme of helical long-period fiber grating for liquid-level sensing," *Appl. Opt.*, vol. 55, no. 34, pp. 9675–9679, Nov. 2016.
[19] I. Del Villar, I. Matías, F. Arregui, and P. Lalanne, "Optimization of sensitivity in long period fiber gratings with overlay deposition," *Opt. Exp.*, vol. 13, no. 1, pp. 56–69, Dec. 2005.
[20] S. Xiang *et al.*, "Helical long-period grating manufactured with a CO_2 laser on multicore fiber," *Opt. Exp.*, vol. 25, no. 9, pp. 10405–10412, 2017.
[21] O. V. Ivanov, "Fabrication of long-period fiber gratings by twisting a standard single-mode fiber," *Opt. Lett.*, vol. 30, no. 24, pp. 3290–3292, Dec. 2005.
[22] D. D. Tian, Y. Q. Liu, and X. B. Cao, "Sensing characteristics of CO_2-laser written helical long-period fiber gratings," in *Proc. 15th Int. Conf. Opt. Commun. Netw.*, Hangzhou, China, Sep. 24–27, 2016, doi: 10.1109/ICOCN.2016.7875747.
[23] R. Q. Lv, Q. Wang, and H. F. Hu, "Fabrication and sensing characterization of thermally induced long period fiber gratings in few mode fibers," *Optik*, vol. 158, pp. 71–77, 2018.
[24] O. V. Ivanov and L. A. Wang, "Wavelength shifts of cladding-mode resonance in corrugated long-period fiber gratings under torsion," *Appl. Opt.*, vol. 42, no. 13, pp. 2264–72, 2003.
[25] W. Shin, Y. L. Lee, and B. A. Yu, "Spectral characterization of helical long-period fiber gratings in photonic crystal fibers," *Opt. Commun.*, vol. 282, no. 17, pp. 3456–3459, Sep. 2009.
[26] S. Cuiting, G. Tao, and H. Jiang, "High sensitive direction torsion sensor based on a segmented long-period fiber grating," *IEEE Photon. Technol. Lett.*, vol. 29, no. 24, pp. 2179–2182, Dec. 2017.
[27] H. Jung, W. Shin, and J. K. Kim, "Bending and strain sensitivities in a helicoidal long-period fiber grating," *IEEE Photon. Technol. Lett.*, vol. 21, no. 17, pp. 1232–1234, Sep. 2009.